Supplementary Information for
"Intertwined Weyl phases emergent from higher-order topology and unconventional Weyl fermions via crystalline symmetry"

W. B. Rui,[1] Zhen Zheng,[1] Moritz M. Hirschmann,[2] Song-Bo Zhang,[3] Chenjie Wang,[1] and Z. D. Wang[1]

[1] *Department of Physics and HKU-UCAS Joint Institute for Theoretical and Computational Physics at Hong Kong,*
The University of Hong Kong, Pokfulam Road, Hong Kong, China
[2] *Max Planck Institute for Solid State Research, Heisenbergstrasse 1, D-70569 Stuttgart, Germany*
[3] *Institute for Theoretical Physics and Astrophysics,*
University of Würzburg, D-97074 Würzburg, Germany

In this Supplementary Information file, we discuss the symmetries in intertwined double-Weyl phases (Supplementary Note 1), derive the effective boundary Hamiltonian (Supplementary Note 2), explain the experimental setup for realizing the intertwined double-Weyl phases (Supplementary Note 3), and briefly discuss the generalization to intertwined triple-Weyl phases (Supplementary Note 4).

Supplementary Note 1.   SYMMETRIES IN INTERTWINED DOUBLE-WEYL PHASES

We start with Eq. (6) of the main text, which can be written in the following form,

$$H(\mathbf{k}) = H_0(\mathbf{k}) + m\tau_1\sigma_1, \tag{1}$$

where $H_0(\mathbf{k})$ describes a normal double-Weyl semimetal,

$$H_0(\mathbf{k}) = 2A(\cos k_y - \cos k_x)\tau_3\sigma_1 + 2A\sin k_x \sin k_y \tau_3\sigma_2 + M(\mathbf{k})\tau_3\sigma_3 + \epsilon\tau_0\sigma_3, \tag{2}$$

with $M(\mathbf{k}) = M_0 - 2t(\cos k_x + \cos k_y + \cos k_z)$.

In order to generate Weyl points, time-reversal symmetry ($\mathcal{T}$) has been broken by the introduction of a term ϵ, and thus,

$$\mathcal{T}H_0(k_x, k_y, k_z)T^{-1} \neq H_0(-k_x, -k_y, -k_z), \; \mathcal{T} = \tau_2\sigma_2\mathcal{K}. \tag{3}$$

Here $\mathcal{K}$ is the complex conjugation operator. The system described by the above Hamiltonian is invariant under inversion symmetry ($\mathcal{I}$), and four-fold rotation symmetry (C_4). The symmetry relations are given by,

$$\mathcal{I}H_0(k_x, k_y, k_z)\mathcal{I}^{-1} = H_0(-k_x, -k_y, -k_z), \; \mathcal{I} = \tau_0\sigma_0, \tag{4}$$

$$\hat{C}_4 H_0(k_x, k_y, k_z)\hat{C}_4^{-1} = H_0(k_y, -k_x, k_z), \; \hat{C}_4 = \tau_3\sigma_3. \tag{5}$$

Since the Weyl points are located on the k_z axis, we can do a series expansion around $(k_x, k_y) = (0,0)$, i.e., $\sin k_{x/y} \to k_{x/y}$ and $\cos k_{x/y} \to 1 - k_{x/y}^2/2$. The obtained continuum model from Eq. (2) is written as

$$H_0(k_x, k_y, k_z) = A(k_x^2 - k_y^2)\tau_3\sigma_1 + 2Ak_x k_y \tau_3\sigma_2 + (M + tk_x^2 + tk_y^2 - 2t\cos k_z)\tau_3\sigma_3 + \epsilon\tau_0\sigma_3, \tag{6}$$

where $M = M_0 - 4t$. Using the polar coordinates $k_x = k\cos\theta$, $k_y = k\sin\theta$, it becomes

$$H_0(k, \theta, k_z) = Ak^2 e^{+2i\theta}\tau_3\sigma_- + Ak^2 e^{-2i\theta}\tau_3\sigma_+ + (M + tk^2 - 2t\cos k_z)\tau_3\sigma_3 + \epsilon\tau_0\sigma_3. \tag{7}$$

Under the fourfold rotation operation about the z axis, the Hamiltonian shall satisfy [1]

$$\hat{C}_4 H_0(k, \theta, k_z)\hat{C}_4^{-1} = H_0(k, R_4\theta, k_z), \tag{8}$$

where $R_4\theta = \theta + \pi/2$. Together with Eq. (5), the double-Weyl points are stabilized by the fourfold rotation symmetry.

Supplementary Note 2.   EFFECTIVE BOUNDARY HAMILTONIAN

In this Supplementary Note, we derive the effective boundary Hamiltonian in the direction defined by $\theta = \arctan(k_y/k_x)$ in the $k_x k_y$-plane at a given position on the k_z axis. To calculate the boundary states along any
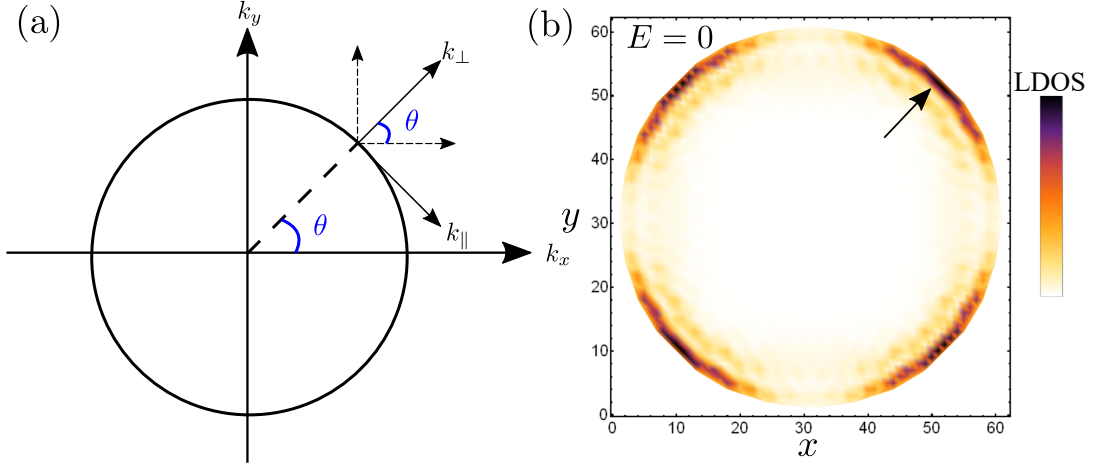
Supplementary Figure 1. (a) Relation between (k_x, k_y) and $(k_\parallel, k_\perp)$ at a given angle θ in the $k_x k_y$-plane [see Fig. 2 (a) in the main text]. The coordinate transformation allows us to calculate the boundary states at any θ at a given position on the k_z axis. (b) Local density of states at zero energy for $k_z = 0$ on a disk geometry with x and y finite, where the higher-order topology manifests itself as the corner modes, as indicated by the black arrow.

direction, as shown in Supplementary Figure 1 (a), we first transform the coordinates from (k_x, k_y) to $(k_\parallel, k_\perp)$. The relation between $(k_\parallel, k_\perp)$ and (k_x, k_y) is given by

$$\begin{pmatrix} k_x \\ k_y \end{pmatrix} = \begin{pmatrix} \sin\theta & \cos\theta \\ -\cos\theta & \sin\theta \end{pmatrix} \begin{pmatrix} k_\parallel \\ k_\perp \end{pmatrix}. \tag{9}$$

After the coordinate transformation, the resulting Hamiltonian (without higher-order term $m\tau_1\sigma_1$) from Eq. (6) reads

$$H_0(k_\parallel, k_\perp, k_z) = \begin{pmatrix} \Delta_{\mathrm{u}} + tk_\perp^2 & -e^{-2i\theta}A(k_\parallel - ik_\perp)^2 & 0 & 0 \\ -e^{+2i\theta}A(k_\parallel + ik_\perp)^2 & -(\Delta_{\mathrm{u}} + tk_\perp^2) & 0 & 0 \\ 0 & 0 & -(\Delta_{\mathrm{d}} + tk_\perp^2) & e^{-2i\theta}A(k_\parallel - ik_\perp)^2 \\ 0 & 0 & e^{+2i\theta}A(k_\parallel + ik_\perp)^2 & (\Delta_{\mathrm{d}} + tk_\perp^2) \end{pmatrix}, \tag{10}$$

where $\Delta_{\mathrm{u}} = M + tk_\parallel^2 - 2t\cos k_z + \epsilon$ and $\Delta_{\mathrm{d}} = M + tk_\parallel^2 - 2t\cos k_z - \epsilon$. The above Hamiltonian is in a block-diagonal form, which enables us to investigate each block separately. First, we focus on the upper block in Eq. (10), which reads

$$h_{\mathrm{u}}(\mathbf{k}) = \begin{pmatrix} \Delta_{\mathrm{u}} + tk_\perp^2 & -e^{-2i\theta}A(k_\parallel - ik_\perp)^2 \\ -e^{+2i\theta}A(k_\parallel + ik_\perp)^2 & -(\Delta_{\mathrm{u}} + tk_\perp^2) \end{pmatrix}. \tag{11}$$

Suppose we have a semi-infinite system in the half plane $x_\perp \leq 0$ with open boundary conditions and with translational symmetry along the $\hat{\mathbf{x}}_\parallel$ and $\hat{\mathbf{z}}$ directions. $k_\parallel$ and k_z are still good quantum numbers but $k_\perp$ is replaced by $k_\perp = -i\partial_\perp$ in the Hamiltonian. We can assume a trial wavefunction for each set of $k_\parallel$ and k_z as

$$\psi_\lambda = e^{ik_\parallel x_\parallel + ik_z z} \begin{bmatrix} \psi_1 \\ \psi_2 \end{bmatrix} e^{\lambda x_\perp}. \tag{12}$$

The corresponding Dirac equation reads $(k_\perp \to -i\lambda)$

$$\begin{pmatrix} \Delta_{\mathrm{u}} - t\lambda^2 & -e^{-2i\theta}A(k_\parallel - \lambda)^2 \\ -e^{+2i\theta}A(k_\parallel + \lambda)^2 & -(\Delta_{\mathrm{u}} - t\lambda^2) \end{pmatrix} \begin{pmatrix} \psi_1 \\ \psi_2 \end{pmatrix} = E \begin{pmatrix} \psi_1 \\ \psi_2 \end{pmatrix}. \tag{13}$$

The secular equation for the eigenenergies can be calculated as

$$\det|h_{\mathrm{u}}(k_\parallel, -i\lambda, k_z) - E| = 0. \tag{14}$$

The equation reads explicitly as

$$(t^2 + A^2)\lambda^4 - 2(t\Delta_{\mathrm{u}} + A^2 k_{\parallel}^2)\lambda^2 + A^2 k_{\parallel}^4 + \Delta_{\mathrm{u}}^2 - E^2 = 0. \tag{15}$$

We can obtain the solution for λ as

$$\lambda_{\alpha}^2 = \frac{1}{(t^2 + A^2)}\left[(t\Delta_{\mathrm{u}} + A^2 k_{\parallel}^2) + (-1)^{\alpha}\sqrt{(t^2 + A^2)E^2 - A^2(\Delta_{\mathrm{u}} - tk_{\parallel}^2)^2}\right]. \tag{16}$$

Here $\alpha = 1, 2$. The corresponding eigenvectors are

$$\psi_{\lambda_{\alpha}} = \begin{pmatrix} e^{-2i\theta}A(k_{\parallel} - \lambda_{\alpha})^2 \\ (\Delta_{\mathrm{u}} - t\lambda_{\alpha}^2) - E \end{pmatrix}, \qquad \text{or} \quad \psi_{\lambda_{\alpha}} = \begin{pmatrix} (\Delta_{\mathrm{u}} - t\lambda_{\alpha}^2) + E \\ -e^{2i\theta}A(k_{\parallel} + \lambda_{\alpha})^2 \end{pmatrix}. \tag{17}$$

Thus, a general wavefunction can be expanded in terms of these eigenvectors.

Using the boundary condition at $x_{\perp} \to \infty$, it is required that $\mathrm{Re}\lambda_{\alpha} > 0$. For the the boundary condition at $x_{\perp} \to 0$, by the following relation $|\psi_{\lambda_1} \quad \psi_{\lambda_2}| = 0$, we get

$$(2k_{\parallel} - \lambda_1 - \lambda_2)E = -(tk_{\parallel}^2 + \Delta_{\mathrm{u}})(\lambda_1 + \lambda_2) + 2k_{\parallel}(\Delta_{\mathrm{u}} + t\lambda_1\lambda_2), \tag{18}$$

$$(2k_{\parallel} + \lambda_1 + \lambda_2)E = -(tk_{\parallel}^2 + \Delta_{\mathrm{u}})(\lambda_1 + \lambda_2) - 2k_{\parallel}(\Delta_{\mathrm{u}} + t\lambda_1\lambda_2). \tag{19}$$

Note that we have $\lambda_1^2 + \lambda_2^2 = (\lambda_1 + \lambda_2)^2 - 2\lambda_1\lambda_2 = 2(t\Delta_{\mathrm{u}} + A^2 k_{\parallel}^2)/(t^2 + A^2)$ from the expression of λ_{α}^2 in Eq. (16). Together with the above equation, we obtain

$$\lambda_1 = \frac{1}{\sqrt{t^2 + A^2}}(Ak_{\parallel} - \sqrt{t\Delta_{\mathrm{u}}}), \tag{20}$$

$$\lambda_2 = \frac{1}{\sqrt{t^2 + A^2}}(Ak_{\parallel} + \sqrt{t\Delta_{\mathrm{u}}}). \tag{21}$$

Plugging λ_{α} into the relation of Eqs. (18) and (19), the eigenenergy is obtained as

$$E = -\frac{A}{\sqrt{t^2 + A^2}}(tk_{\parallel}^2 + \Delta_{\mathrm{u}}) = -\frac{A}{\sqrt{t^2 + A^2}}(2tk_{\parallel}^2 + M - 2t\cos k_z + \epsilon). \tag{22}$$

The eigenstates are obtained as

$$\psi_u = \begin{pmatrix} e^{-2i\theta} \\ \frac{A}{t}(\sqrt{t^2 + A^2} + A) \end{pmatrix}. \tag{23}$$

In the following, we take $t = A = 1$, in accordance with the parameters in our numerical calculation. It is required that $\mathrm{Re}\lambda_{\alpha} > 0$ in order for the wavefunction to decay exponentially away from the boundary. Thus,

$$\lambda_1\lambda_2 = \frac{1}{t^2 + A^2}(A^2 k_{\parallel}^2 - t\Delta_{\mathrm{u}}) > 0. \tag{24}$$

The corresponding k_z shall satisfy $-\arccos\frac{M+\epsilon}{2} < k_z < \arccos\frac{M+\epsilon}{2}$, which lies approximately between the two Weyl points, i.e., $k_z \in (-k_{w2}, k_{w2})$ in Fig. 2 (a) in the main text. Returning to the full 4×4 Hamiltonian, the eigenfunctions for the boundary states in this region are in the form of

$$\psi_u \propto \begin{pmatrix} e^{-2i\theta} \\ \sqrt{2} + 1 \\ 0 \\ 0 \end{pmatrix}, \text{for } k_z \in (-k_{\mathrm{w}2}, k_{\mathrm{w}2}). \tag{25}$$

Note that the contributions from spatial part are neglected here, as they do not affect the main results.

A similar procedure can be obtained for the lower block of

$$h_{\mathrm{d}}(\mathbf{k}) = \begin{pmatrix} -(\Delta_{\mathrm{d}} + tk_\perp^2) & e^{-2i\theta} A(k_\parallel - ik_\perp)^2 \\ e^{+2i\theta} A(k_\parallel + ik_\perp)^2 & (\Delta_{\mathrm{d}} + tk_\perp^2) \end{pmatrix}. \tag{26}$$

The wavefunction is obtained as

$$\psi_{\mathrm{d}} \propto \begin{pmatrix} 0 \\ 0 \\ e^{-2i\theta} \\ \sqrt{2} + 1 \end{pmatrix}, \text{for } k_z \in (-k_{\mathrm{w}1}, k_{\mathrm{w}1}). \tag{27}$$

The boundary states in Eqs. (25) and (27) are both valid in the region of $(-k_{\mathrm{w}1}, k_{\mathrm{w}1}) \cap (-k_{\mathrm{w}2}, k_{\mathrm{w}2})$. For the chosen parameters in numerical calculations, $k_{\mathrm{w}2} < k_{\mathrm{w}1}$, and thus, $(-k_{\mathrm{w}1}, k_{\mathrm{w}1}) \cap (-k_{\mathrm{w}2}, k_{\mathrm{w}2}) = (-k_{\mathrm{w}2}, k_{\mathrm{w}2})$. In this region, we can project the system to the boundary with the normalized eigenvectors, and obtain the following effective boundary Hamiltonian,

$$h_{\mathrm{eff}} = -\frac{1}{\sqrt{2}}[(2k_\parallel^2 - k_{\mathrm{c}}^2)\sigma_3 - m\cos(2\theta)\sigma_1], \text{ for } k_z \in (-k_{\mathrm{w}2}, k_{\mathrm{w}2}), \tag{28}$$

up to a constant term $-1/\sqrt{2}\varepsilon\sigma_0$, where $k_{\mathrm{c}}^2 = 2t\cos k_z - M$.

We can also project the fourfold rotation symmetry operator to the boundary, and obtain $\hat{c}_4 = \sigma_3$. The higher-order term satisfies this symmetry, i.e., $\hat{c}_4[m\cos(2\theta)\sigma_1]\hat{c}_4^{-1} = m\cos[2(\theta + \pi/2)]\sigma_1$. Note that the rotation symmetry does not allow constant terms that are proportional to σ_2 after projection. The symmetry enforces the following condition at the boundary

$$m\cos[2(\theta + \pi/2)] = -m\cos(2\theta). \tag{29}$$

This implies that there must be gapless states when going from θ to $\theta + \pi/2$, resulting in higher-order topology. In Fig. 1 (b), the corner states are shown by calculating the local density of states at zero energy, in the higher-order topology region at $k_z = 0 \in (-k_{\mathrm{w}2}, k_{\mathrm{w}2})$. These corner states leads to hinge Fermi arcs as shown in Fig. 1(b) in the main text.

Supplementary Note 3. PROPOSAL FOR EXPERIMENTAL REALIZATION

We consider the atomic Fermi gas trapped in a 2D bilayer optical lattice, in which the layer index is denoted as $\lambda = 1, 2$. The system is governed by the following Hamiltonian,

$$H = H_{\mathrm{hop}} + H_{\mathrm{soc}} + H_{\mathrm{os}}. \tag{30}$$

The first term H_{hop} describes the nearest-neighbor hopping,

$$H_{\mathrm{hop}} = -\sum_\lambda \sum_j \sum_{\eta=x,y} \sum_{\nu=\uparrow\downarrow} t c_{j\nu\lambda}^\dagger c_{j+e_\eta,\nu,\lambda} - \sum_j \sum_\nu t_z c_{j\nu1}^\dagger c_{j\nu2} + H.c. \tag{31}$$

where $c_{j\nu\lambda}$ denotes the annihilation operator of the atom with spin-ν on j-th site of the λ-th layer, and $e_{x,y,z}$ denotes the unit vector.

The second term H_{soc} describes the spin-orbit coupling. We engineer this term by coupling opposite spins via laser fields of three modes: $M_1(\mathbf{r}) = iM_1 \sin(k_{\mathrm{L}}x)\sin(k_{\mathrm{L}}y)$, $M_2(\mathbf{r}) = M_2\cos(k_{\mathrm{L}}x)\cos(\mathcal{N}k_{\mathrm{L}}y)\cos(k_{\mathrm{L}}z)$, and $M_2'(\mathbf{r}) = -M_2\cos(\mathcal{N}k_{\mathrm{L}}x)\cos(k_{\mathrm{L}}y)\cos(k_{\mathrm{L}}z)$. Here $k_{\mathrm{L}} = \pi/d$ and d denotes the lattice constant. $\mathcal{N}$ is an arbitrary odd number greater than 1 (i.e. $\mathcal{N} = 3, 5, 7, \cdots$). Due to the odd parity of $M_1(\mathbf{r})$ in the xy-plane for either x and y, the on-site and nearest-neighbor (NN) terms vanish, leaving the next-NN terms dominant [2]:

$$H_{\mathrm{soc}}^{(1)} = \sum_\lambda \sum_j \sum_{\nu\nu'} (-1)^{j_x+j_y} A_1[\sigma_2]_{\nu\nu'}(c_{j\nu\lambda}^\dagger c_{j+e_x-e_y,\nu',\lambda} - c_{j\nu\lambda}^\dagger c_{j+e_x+e_y,\nu',\lambda}) + H.c. \tag{32}$$

where $iA_1 = \int M_1(\mathbf{r})W^*(\mathbf{r})W(\mathbf{r} + de_x + de_y)d\mathbf{r}$. The modes $M_2(\mathbf{r})$ and $M_2'(\mathbf{r})$ can introduce both the on-site and NN terms. However, due to the crystal symmetry, the Wannier wave function of atoms on each site is isotropic in

the x, y, and z directions. Since there exists difference in sign between $M_2(\mathbf{r})$ and $M_2'(\mathbf{r})$, both the on-site and the z-directional NN terms cancel out, leaving the NN terms in the xy-plane dominant:

$$H_{\text{soc}}^{(2)} = \sum_\lambda \sum_j \sum_{\nu\nu'} (-1)^\lambda (-1)^{j_x+j_y} A_2 [\sigma_1]_{\nu\nu'} [c_{j\nu\lambda}^\dagger c_{j+e_y,\nu',\lambda} - c_{j\nu\lambda}^\dagger c_{j+e_x,\nu',\lambda}] + H.c. \tag{33}$$

where we have denoted $A_2 = \int [M_2(\mathbf{r}) - M_2'(\mathbf{r})] W^*(\mathbf{r}) W(\mathbf{r} + de_y) d\mathbf{r}$. By combining Eqs. (32) and (33), H_{soc} is given as

$$H_{\text{soc}} = H_{\text{soc}}^{(1)} + H_{\text{soc}}^{(2)}. \tag{34}$$

For simplicity, we can tune $2A_1 = A_2 = A$ in experiments.

The last term H_{os} describes the on-site energy,

$$H_{\text{os}} = \sum_\lambda \sum_j \sum_{\nu\nu'} \Gamma_\lambda(\phi) [\sigma_3]_{\nu\nu'} c_{j\nu\lambda}^\dagger c_{j\nu'\lambda}. \tag{35}$$

It can be engineered by the Zeeman split of hyperfine levels and assigned with a tunable cyclical parameter ϕ,

$$\Gamma_\lambda(\phi) = M_0 + (-1)^\lambda \epsilon - 2t \cos(\phi). \tag{36}$$

We make the following operator transformation which preserves the anti-commutation of fermionic operators,

$$c_{j\uparrow 1} \rightarrow c_{j\uparrow 1}, \qquad c_{j\downarrow 1} \rightarrow (-1)^{j_x+j_y} c_{j\downarrow 1}, \qquad c_{j\uparrow 2} \rightarrow c_{j\downarrow 2}, \qquad c_{j\downarrow 2} \rightarrow (-1)^{j_x+j_y} c_{j\uparrow 2}. \tag{37}$$

In the base $c = (c_{\uparrow 1}, c_{\downarrow 1}, c_{\uparrow 2}, c_{\downarrow 2})^T$, Hamiltonian (30) is then rewritten as

$$H = \sum_j \Big[-\sum_{\eta=x,y} t\tau_3\sigma_3 c_j^\dagger c_{j+e_\eta} + A\tau_3\sigma_1(c_j^\dagger c_{j+e_y} - c_j^\dagger c_{j+e_x}) + \frac{A}{2}\tau_3\sigma_2(c_j^\dagger c_{j+e_x-e_y} - c_j^\dagger c_{j+e_x+e_y}) + H.c. \Big]$$
$$+ \Gamma_\lambda(\phi)\tau_3\sigma_3 c_j^\dagger c_j - t_z\tau_1\sigma_1 c_j^\dagger c_j. \tag{38}$$

We remark that the higher-order topological term $\tau_1\sigma_1$ naturally originates from the hopping in the z direction. Hereafter, we denote $-t_z \equiv m$ to be consistent with formulas in the main text.

Since ϕ is manually controllable, we can treat it as an artificial dimension of the z axis under periodic boundary conditions along this direction. The 2D momentum space (k_x, k_y) is then mapped into a 3D parameterized space (k_x, k_y, ϕ). By transforming Eq. (38) into the momentum space, we can obtain the effective Hamiltonian that is identical to the model in the main text:

$$H(\mathbf{k}) = 2A[\cos(k_y d) - \cos(k_x d)]\tau_3\sigma_1 + 2A\sin(k_x d)\sin(k_y d)\tau_3\sigma_2 + M(\mathbf{k})\tau_3\sigma_3 + \epsilon\tau_0\sigma_3 + m\tau_1\sigma_1, \tag{39}$$

where $M(\mathbf{k}) = M_0 - 2t \sum_{\eta=k_x,k_y,\phi} \cos(\eta d)$.

We are interested in Fermi-arc topology on the surfaces that are parallel to ϕ (i.e., k_z) direction. Using the time-of-flight images [3, 4], the Fermi arc surface states at a specific surface orientation may be determined, by measuring the density on boundaries of the atomic cloud parallel to the expansion direction. In order to process the measurement on a specific surface termination normal to the xy-plane, one can switch off the trap of atoms in one direction (at an angle θ to the x-axis), while keeping the confinement in the relative perpendicular direction. This is practically feasible because the magneto-optic trap and the optical lattice trap are separately generated, and thus, this provides provides the possibility for artificially controlling the expansion direction in the xy-plane.

Supplementary Note 4. GENERALIZATION TO INTERTWINED TRIPLE-WEYL PHASES

The intertwined triple-Weyl phases could be constructed similarly to intertwined double-Weyl phases. By a straightforward generalization from the continuum model in Eq. (6), the low energy effective model for the intertwined triple-Weyl phases is

$$H_0(k_x, k_y, k_z) = Ak_x(k_x^2 - 3k_y^2)\tau_3\sigma_1 + Ak_y(3k_x^2 - k_y^2)\tau_3\sigma_2 + (M + tk_x^2 + tk_y^2 - 2t\cos k_z)\tau_3\sigma_3 + \epsilon\tau_0\sigma_3. \tag{40}$$

Time-reversal symmetry is broken by the term $\epsilon\tau_0\sigma_3$, which can be seen by $\mathcal{T}\epsilon\tau_0\sigma_3 T^{-1} = -\epsilon\tau_0\sigma_3$. Thus,

$$\mathcal{T} H_0(k_x, k_y, k_z) T^{-1} \neq H_0(-k_x, -k_y, -k_z), \ \mathcal{T} = \tau_1\sigma_1\mathcal{K}. \tag{41}$$

The inversion symmetry is still preserved,

$$\mathcal{I}H_0(k_x, k_y, k_z)\mathcal{I}^{-1} = H_0(-k_x, -k_y, -k_z),\ \mathcal{I} = \tau_3\sigma_3. \tag{42}$$

Using the substitution of $k_x = k\cos\theta, k_y = k\sin\theta$, the above Hamiltonian becomes,

$$H_0(k, \theta, k_z) = Ak^3 e^{+3i\theta}\tau_3\sigma_- + Ak^3 e^{-3i\theta}\tau_3\sigma_+ + (M + tk^2 - 2t\cos k_z)\tau_3\sigma_3 + \epsilon\tau_0\sigma_3. \tag{43}$$

The Hamiltonian is protected by the sixfold rotation symmetry,

$$\hat{C}_6 H_0(k, \theta, k_z)\hat{C}_6^{-1} = H_0(k, R_6\theta, k_z),\ \hat{C}_6 = \tau_3\sigma_3 \text{ and } R_6\theta = \theta + \frac{\pi}{3}. \tag{44}$$

We are interested in symmetry allowed terms that could generate higher-order topology. It is found that $m\tau_1\sigma_1$ is again invariant under C_6 symmetry as

$$\hat{C}_6 m\tau_1\sigma_1 \hat{C}_6^{-1} = m\tau_1\sigma_1. \tag{45}$$

Thus, the Hamiltonian for intertwined triple-Weyl phases could be constructed as

$$H(k_x, k_y, k_z) = Ak_x(k_x^2 - 3k_y^2)\tau_3\sigma_1 + Ak_y(3k_x^2 - k_y^2)\tau_3\sigma_2 + (M + tk_x^2 + tk_y^2 - 2t\cos k_z)\tau_3\sigma_3 + \epsilon\tau_0\sigma_3 + m\tau_1\sigma_1. \tag{46}$$

The local density of states on surface with different orientations are calculated in Figs. 1(g-i) in the main text.

---

[1] C. Fang, M. J. Gilbert, X. Dai, and B. A. Bernevig, Phys. Rev. Lett. **108**, 266802 (2012).
[2] X.-J. Liu, K. T. Law, and T. K. Ng, Phys. Rev. Lett. **112**, 086401 (2014).
[3] D.-W. Zhang, Y.-Q. Zhu, Y. X. Zhao, H. Yan, and S.-L. Zhu, Adv. Phys. **67**, 253 (2018).
[4] L. Wang, A. A. Soluyanov, and M. Troyer, Phys. Rev. Lett. **110**, 166802 (2013).